

Ornstein-Uhlenbeck Adaptation as a Mechanism for Learning in Brains and Machines

Jesús García Fernández¹, Nasir Ahmad¹, and Marcel van Gerven¹

¹Department of Machine Learning and Neural Computing, Donders Institute for Brain, Cognition and Behaviour, Radboud University, Nijmegen, the Netherlands

Abstract

Learning is a fundamental property of intelligent systems, observed across biological organisms and engineered systems. While modern intelligent systems typically rely on gradient descent for learning, the need for exact gradients and complex information flow makes its implementation in biological and neuromorphic systems challenging. This has motivated the exploration of alternative learning mechanisms that can operate locally and do not rely on exact gradients. In this work, we introduce a novel approach that leverages noise in the parameters of the system and global reinforcement signals. Using an Ornstein-Uhlenbeck process with adaptive dynamics, our method balances exploration and exploitation during learning, driven by deviations from error predictions, akin to reward prediction error. Operating in continuous time, Ornstein-Uhlenbeck adaptation (OUA) is proposed as a general mechanism for learning dynamic, time-evolving environments. We validate our approach across diverse tasks, including supervised learning and reinforcement learning in feedforward and recurrent systems. Additionally, we demonstrate that it can perform meta-learning, adjusting hyperparameters autonomously. Our results indicate that OUA provides a viable alternative to traditional gradient-based methods, with potential applications in neuromorphic computing. It also hints at a possible mechanism for noise-driven learning in the brain, where stochastic neurotransmitter release may guide synaptic adjustments.

1 Introduction

One of the main properties of any intelligent system is that it has the capacity to learn. This holds for biological systems, ranging from bacteria and fungi to plants and animals [16, 20, 41, 49], as well as for engineered systems as developed by artificial intelligence researchers and control theorists [58, 28, 9].

Modern intelligent systems, such as those used in machine learning, typically rely on gradient descent for learning, which adjusts parameters based on the minimization of error gradients [31, 64, 48]. While gradient-based methods have driven significant advances in AI [28], their reliance on exact gradients, precise parameter updates, and complex information pathways makes them difficult to implement in biological and neuromorphic systems. Biological learning likely relies on different mechanisms, as organisms often lack the exact gradient information and centralized control that gradient descent requires [30, 67]. These same issues have also impeded progress in implementing learning algorithms on neuromorphic hardware, which aims to mimic the distributed, energy-efficient processing seen in biological systems [37, 39].

For this reason, alternative learning principles have been proposed for both rate-based [44, 7, 50, 5, 66] and spike-based models [35, 4, 21, 45]. A specific class of methods leverages inherent noise present in biological systems to facilitate learning. These perturbation-based methods [56, 68, 65] adjust the system's parameters based on noise effects and global reinforcement signals, offering gradient-free, local learning suitable for biological or neuromorphic systems. Within this framework, node perturbation methods [19, 22, 69, 65, 18, 11, 17, 29, 38] considers noise in the

nodes, while weight perturbation methods [26, 32, 71, 10, 12] focus on noisy parameters, akin to stochastic neurotransmitter release in biological synapses.

In this work, we propose a learning mechanism that may offer insights into biological learning processes while also enabling learning in engineered systems. Similar to the latter approaches, it leverages inherent noise, specifically in the system's parameters, combined with global reinforcement signals. At its core, the method uses an Ornstein-Uhlenbeck (OU) process [61, 13] with an adaptive mechanism, enabling both exploration and exploitation during learning. The reinforcement signal is based on deviations from error predictions, resembling a reward prediction error (RPE) that is thought to be involved in biological learning [52]. Our method operates in continuous time, with parameter updates defined through differential equations, making it compatible with continual learning in dynamic, time-evolving environments [27]. Due to the simple and local nature of the proposed mechanism, it is ideally suited for implementing learning on neuromorphic hardware.

We validate our approach across various experiments, including feedforward and recurrent systems, covering input-output mappings, control tasks, and a real-world weather forecasting task, all within a continuous-time framework. Additionally, we demonstrate that the method can be extended for meta-learning by learning the system hyperparameters. Finally, we discuss implications and extensions of our approach.

2 Methods

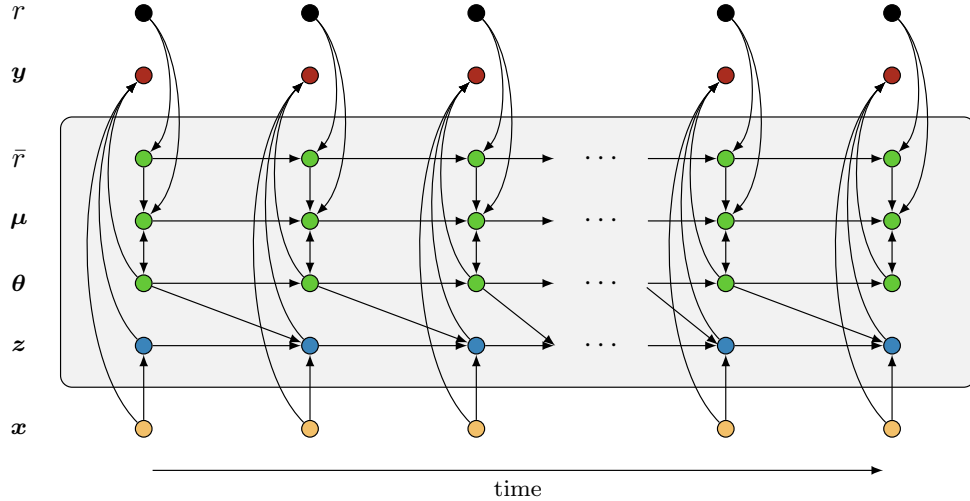


Figure 1: Dependency structure of the variables that together determine Ornstein-Uhlenbeck adaptation. The average reward estimate \bar{r} depends on rewards r that result from the outputs y generated by the model. The gray box indicates the latent variables that together determine the input-output mapping from x to y . Variables z in blue are related to inference whereas variables (\bar{r}, μ, θ) in green are related to learning.

2.1 Inference

Consider an inference problem, where the goal is to map inputs $\mathbf{x}(t) \in \mathbb{R}^m$ to outputs $\mathbf{y}(t) \in \mathbb{R}^k$ for $t \in \mathbb{R}^+$. This problem can be formulated in most general terms as a stochastic state space model

$$d\mathbf{z} = f_{\theta}(\mathbf{z}, \mathbf{x}) dt + d\zeta \quad (1)$$

$$\mathbf{y} = g_{\theta}(\mathbf{z}, \mathbf{x}) + \epsilon \quad (2)$$

where we suppress the time index t for all variables from our notation for readability. Here, $\boldsymbol{\theta} \in \mathbb{R}^n$ are (learnable) parameters, $\mathbf{z} \in \mathbb{R}^d$ is a latent process, f and g are nonlinear functions parameterized by $\boldsymbol{\theta}$, ζ is process noise, and ϵ is observation noise. We assume that we integrate the process from some initial time t_0 up to some time horizon T . We also refer to Equation (1) as a (latent) neural stochastic differential equation [60], where ‘neural’ refers to the use of learnable parameters $\boldsymbol{\theta}$.

2.2 Reward prediction

To learn how to adapt, we assume the existence of a global scalar reward signal r , providing instantaneous feedback about the efficacy of the system’s output y . The question is how to change the parameters such as to maximize the cumulative reward or return

$$G(t) = \int_{t_0}^t r(\tau) d\tau \quad (3)$$

as $t \rightarrow T$. We may formulate the return as part of the dynamics using $dG = r dt$ with $G_0 = 0$, where $G_0 = G(t_0)$ denotes the initial state. To be able to learn, the agent is assumed to maintain a moving average of the reward [63] according to

$$d\bar{r} = \rho(r - \bar{r}) dt \quad (4)$$

This is equivalent to applying a low-pass filter to the reward with time-constant $1/\rho$. We also refer to $\delta_r = r - \bar{r}$ as the reward prediction error (RPE), which can be interpreted as a global dopaminergic neuromodulatory signal that is essential for learning in biological systems [52].

2.3 Learning

Often, learning is viewed as separate from inference. Here, in contrast, we cast learning and inference as processes that co-evolve over time by making the parameters $\boldsymbol{\theta}$ part of the system dynamics. In this sense, the only distinction between learning and inference is that the former evolves at a slower time scale compared to the latter.

The question remains how we can set up learning dynamics such that the parameters adapt towards a more desirable state. To this end, we define learning as a stochastic process evolving forward in time. Specifically, let us assume that parameter dynamics are given by an Ornstein-Uhlenbeck (OU) process

$$d\boldsymbol{\theta} = \lambda(\boldsymbol{\mu} - \boldsymbol{\theta}) dt + \boldsymbol{\Sigma} d\mathbf{W} \quad (5)$$

with $\boldsymbol{\mu}$ the mean parameter, λ the rate parameter, $\boldsymbol{\Sigma} = \text{diag}(\sigma_1, \dots, \sigma_n)$ the diffusion matrix, and $\mathbf{W} = (W_1, \dots, W_n)^\top$ a stochastic process, which we take here to be a multivariate Wiener process. The idea is that the first term on the right-hand side of (5) provides stability as it is mean-reverting, whereas the second term provides a random force which explores new parameter values. That is, we define the classical exploration-exploitation dilemma at the level of individual parameters.

If we would just run (5) forward in time, no learning would occur since the parameters would simply drift about the parameter mean $\boldsymbol{\mu}$. We can however induce adaptation by defining the mean itself in terms of an ordinary differential equation

$$d\boldsymbol{\mu} = \eta\delta_r(\boldsymbol{\theta} - \boldsymbol{\mu}) dt \quad (6)$$

where η is the rate parameter and $\delta_r = r - \bar{r}$ is the RPE.

Since (5) defines learning dynamics in terms of an Ornstein-Uhlenbeck process, we refer to our proposed learning mechanism as Ornstein-Uhlenbeck adaptation (OUA). As we will see, OUA shifts the mean towards more favorable values of $\boldsymbol{\theta}$, thereby realizing learning in neuromorphic systems.

2.4 Experimental validation

To test OUA as a mechanism for learning, we consider a number of different settings. First, we consider a single-parameter model, to gain insight into the learning dynamics. Second, we consider recurrent and multiple-parameter models to test parameter interactions. Third, we consider a real-world weather prediction task, where the aim is to predict temperature 24 hours forward in time based on current measurements of temperature, humidity, wind speed, wind bearing (sine and cosine components) and atmospheric pressure. The dataset used in this task contains hourly recordings for Szeged, Hungary area, between 2006 and 2016¹. Outliers were removed using linear interpolation and data was either standardized or whitened prior to further processing. Fourth, we consider a control task, where the aim is to keep the position and velocity of a particle subject to Brownian motion close to zero. We refer to this control task as the stochastic double integrator problem [46]. Finally, we consider meta-learning, where hyper-parameters are adapted using our learning approach.

To implement OUA, we resort to numerical simulation. Equations (1), (2), (4), (5) and (6) together define a coupled system consisting of stochastic and ordinary differential equations. Here, (1) and (2) implement inference whereas (4), (5) and (6) implement learning. To integrate the system from the initial time t_0 to the time horizon T , we used an Euler-Heun solver implemented in the Python `Diffra`x package [25]. In each experiment, the step size for numerical integration was set to $\Delta t = 0.05$. To interpolate inputs for the weather prediction task across the time window of interest, we used cubic Hermite splines with backward differences [42].

To ensure reproducibility, all scripts needed to replicate the results presented in this study are available via <https://github.com/artcogsys/OUA>.

3 Results

3.1 Learning a single-parameter model

To facilitate analysis let us start by examining learning dynamics in for a non-linear model consisting of one learnable parameter θ . We assume that

$$y = g_\theta(x) = \tanh(\theta x) \quad (7)$$

with input x and output y . That is, we do not make use of a latent state z . The input is given by a sinusoid $x(t) = \sin(10t)$ and the reward is given by $r = -(y - y^*)^2$. The target output is given by $y^* = \tanh(\theta^* x)$ where the ground-truth parameter $\theta^* = 1$ is assumed to be given by some teacher. That is, we focus on supervised learning of a non-linear input-output mapping. Learning dynamics for the single-parameter model are given by

$$d\theta = \lambda(\mu - \theta) dt + \sigma dW \quad (8)$$

$$d\mu = \eta \delta r(\theta - \mu) dt \quad (9)$$

with W a standard Wiener process.

Figure 2 demonstrates the dynamics of a single-parameter model, repeated using 15 different random seeds. Figures 2a and 2b show that θ and μ move from their initial state towards their optimal (ground-truth) state. Figures 2c shows that the reward prediction error decreases over time. Figure 2d shows that more reward is accumulated as learning progresses. Results show that the return received with learning is substantially higher than the return received without learning. Variability in the return is associated with the time it takes for the parameter to converge to the optimum in individual runs.

It is also instructive to analyse how sensitive parameter convergence is to the choice of hyper-parameters. Figure 3 shows how the choice of hyper-parameters influences learning dynamics. For all hyper-parameters we see a clear peak in the return G , except for ρ since the true average reward

¹Data can be obtained from <https://www.kaggle.com/datasets/budincsevity/szeged-weather/>.

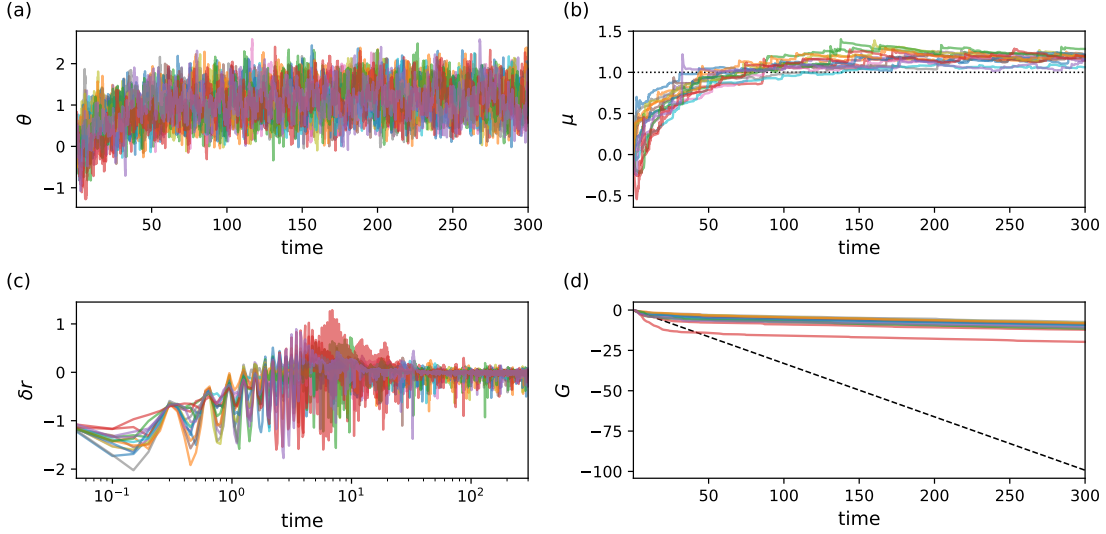


Figure 2: Dynamics of a single-parameter model for 15 different seeds with $\rho = \lambda = \eta = 1$ and $\sigma = 0.5$. Initial conditions are given by $\bar{r}_0 = -1$, $\theta_0 = \mu_0 = 0$. The ground-truth parameter value is given by $\theta^* = 1$. Initial conditions and optimal conditions are indicated by dashed and dotted lines, respectively. a) Dynamics of the parameter θ . b) Dynamics of the mean μ . c) Dynamics of the reward prediction error δr . d) Return G as a function of time. Higher is better. The dashed line denotes the return when θ is fixed to its initial state θ_0 whereas the dotted line indicates the return obtained using the optimal parameter θ^* .

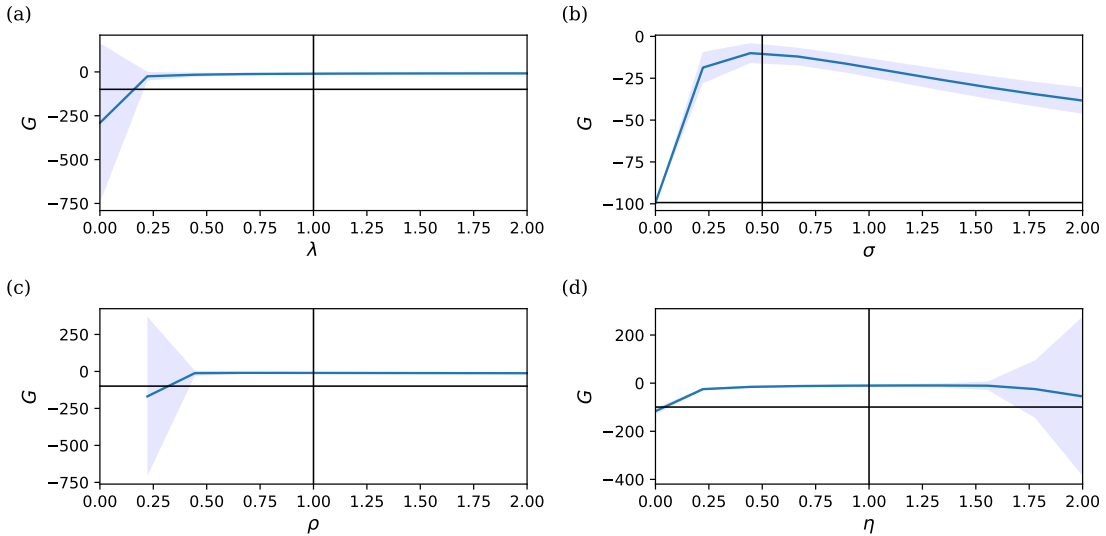


Figure 3: Parameter sensitivity expressed in terms of the cumulative reward G evaluated at the time horizon T . Vertical lines indicate the chosen value of the hyper-parameter when learning the single-parameter model. Horizontal lines indicate the return in the absence of learning. Results averaged over 15 runs. a) Dependence of G on λ . b) Dependence of G on σ . c) Dependence of G on ρ . d) Dependence of G on η .

is equal to the initial estimate of $\bar{r}_0 = 0$. Missing data for low values of ρ are due to numerical

instability for these values. Even for high noise levels σ , we still observe effective learning.

3.2 Learning in recurrent systems

Whereas the previous analysis focused on learning linear input-output mappings, we here focus on learning a non-linear dynamical system given by

$$\begin{aligned} dz &= (f(\theta_1 z + \theta_2 x) - z) dt \\ y &= \theta_3 z \end{aligned} \quad (10)$$

with input x , latent state z and output y . The system (10) could also be interpreted as a continuous-time recurrent neural network (CTRNN) or a latent ordinary differential equation (ODE). The reward is given by $r = -(y - y^*)^2$ where y^* is generated by (10) using ground truth parameters $\theta^* = (\theta_1, \theta_2, \theta_3) = (1, 1, 1)$. This system requires fast dynamics in z and slow dynamics in θ . We demonstrate OUA's capability to learn the parameters of a recurrent model by training it on a 1D input-output mapping.

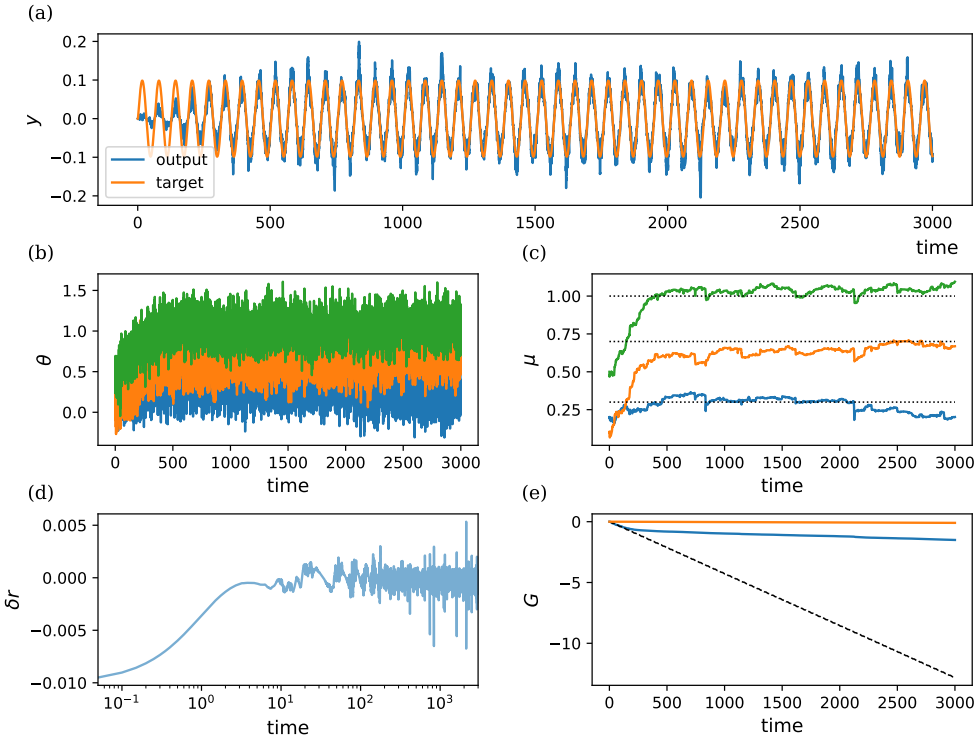


Figure 4: Dynamics of a model consisting of parameters $\theta = [\theta_1, \theta_2, \theta_3]$ with $\rho = \lambda = 1$, $\eta = 50$ and $\sigma = 0.2$. Initial conditions are given by $\bar{r}_0 = -0.1$ and $\theta_0 = [0.2, 0.1, 0.5]$. Ground-truth parameter values are given by $\theta^* = [0.3, 0.7, 1.0]$. Initial conditions and optimal conditions are indicated by dashed and dotted lines, respectively. b) Dynamics of the parameters θ . c) Dynamics of the means μ . d) Dynamics of the reward prediction error $\delta r = r - \bar{r}$. Time variable shown on a logarithmic axis to visualise initial convergence. e) Return G as a function of time. Higher is better. The blue line indicates the return during parameter learning. The dashed line denotes the return when θ are fixed to their initial values θ_0 . The orange line indicates the return obtained when we fix parameters to the final mean parameters $\theta(t) = \mu(T)$ and use these during inference.

Figure 4 illustrates the dynamics of a minimalist recurrent model with only three parameters: input to latent space, recurrent connections within the latent space, and latent space to output. In Figure 4a, the system’s output y gradually aligns with the target output as learning advances. Figure 4c depicts the learning of μ , with the optimal values indicated by dotted lines how μ is learned, depicting its optimal values with dotted lines. Figure 4e shows that more reward is accumulated as learning progresses. Results show that the return received with learning is substantially higher than the return received without learning.

3.3 Learning a multi-parameter model

The question remains whether or not effective learning remains possible in case of multiple parameters $\boldsymbol{\theta} = (\theta_1, \dots, \theta_n)^\top$. To address this question, assume that

$$y = g_{\boldsymbol{\theta}}(\mathbf{x}) = \tanh(\boldsymbol{\theta}^\top \mathbf{x}) \quad (11)$$

with input $\mathbf{x} = (x_1, \dots, x_n)^\top$ and output y . We assume that the input is given by multiple sine waves such that $x_i(t) = \sin(it + (i-1)2\pi/n)$ for $1 \leq i \leq n$. The reward is given by $r = -(y - y^*)^2$ with target $y^* = \tanh((\boldsymbol{\theta}^*)^\top \mathbf{x})$ and ground-truth parameters are given by $\boldsymbol{\theta}^* = (3.3, 1.1, 0.0, -0.3, -1.5, -2.4)^\top$. Finally, learning dynamics are given by

$$d\boldsymbol{\theta} = \lambda(\boldsymbol{\mu} - \boldsymbol{\theta}) dt + \boldsymbol{\Sigma} d\mathbf{W} \quad (12)$$

$$d\boldsymbol{\mu} = \eta \delta r (\boldsymbol{\theta} - \boldsymbol{\mu}) dt \quad (13)$$

with $\boldsymbol{\Sigma} = \sigma \mathbf{I}$ and $\mathbf{W} = (W_1, \dots, W_n)^\top$ a multivariate standard Wiener process.

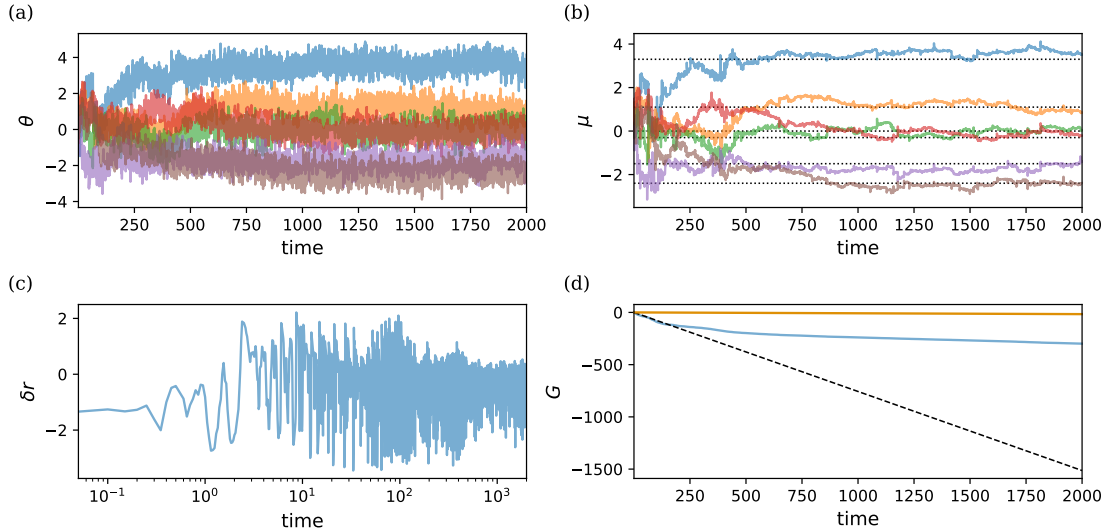


Figure 5: Dynamics of a model consisting of six parameters $\boldsymbol{\theta} = (\theta_1, \dots, \theta_6)^\top$ with $\rho = \lambda = \eta = 1$ and $\sigma = 0.5$. Initial conditions are given by $\bar{r}_0 = -1$ and $\boldsymbol{\theta}_0 = \boldsymbol{\mu}_0 = \mathbf{0}$. Ground-truth parameter values are given by $\boldsymbol{\theta}^* = (1, 1, 0, 0, -1, -1)^\top$. Initial conditions and optimal conditions are indicated by dashed and dotted lines, respectively. a) Dynamics of the parameters $\boldsymbol{\theta}$. b) Dynamics of the means $\boldsymbol{\mu}$. c) Dynamics of the reward prediction error $\delta r = r - \bar{r}$. Time variable shown on a logarithmic axis to visualise initial convergence. d) Return G as a function of time. Higher is better. The blue line indicates the return during parameter learning. The dashed line denotes the return when $\boldsymbol{\theta}$ is fixed to its initial state $\boldsymbol{\theta}_0$ whereas the dotted line indicates the return obtained using the optimal parameters $\boldsymbol{\theta}^*$. The orange line indicates the return obtained when we fix parameters to the final mean parameters $\boldsymbol{\theta}(t) = \boldsymbol{\mu}(T)$ and use these during inference.

Figure 5 shows that effective learning can still be achieved in case of multiple parameters. Figure 5a shows that, as learning progresses, the parameters are correctly dissociated with two parameter values converging to positive values, two parameter values to zero values and two parameters to negative values. This is more prominently visible in the mean parameters μ , as shown in Fig. 5b. Figure 5c shows that the reward differential decreases over time, indicating effective learning since the reward approaches the average reward. This is also reflected by the return in Fig. 5d.

Note that we may also choose to use the final means μ as the parameters estimated after learning. While this steps away from the continual learning setting, it is of importance when deploying trained systems in real-world applications. The orange line in Fig. 5d shows that this indeed provides optimal performance.

3.4 Weather prediction task

We now apply our approach to a real-world weather prediction task. Inputs \mathbf{x} are given by current temperature, humidity, wind speed, sine of wind direction angle, cosine of wind direction angle and humidity. The goal is to learn to predict the temperature 24 hours later. Our setup is the same as for the multiple-parameter analysis, except that y^* now denotes the target 24-hour ahead temperature and the predicted temperature is given by $y = \theta^\top \mathbf{x}$. To validate test performance, a separate segment of the weather dataset was used. Finally, motivated by recent work which shows that input decorrelation is beneficial for learning [2, 1], input features were considered with and without ZCA whitening [3].

Figure 6a-c shows the learning dynamics for this task. Figure 6d shows that, during training, the model learns to improve the return. Figure 6e shows a scatter plot for true versus predicted 24-hour ahead temperature before training (orange) and after training, either with ZCA (blue) or without ZCA (green). The final mean values $\mu(T)$ were used as the parameters $\theta(t)$ when performing inference on separate test data. Results show that accurate prediction is achieved with a Pearson correlation of 0.84 and 0.79 between true and predicted 24h-ahead temperature, with and without ZCA, respectively. Figure 6f shows these final mean values, indicating that the current temperature mostly determines the prediction outcome.

3.5 Learning to control a stochastic double integrator

Next, we consider the stochastic double integrator (SDI) control task. This is a more challenging setting compared to the supervised learning case considered so far since the output of the agent will affect the controlled system and thereby the observations of the agent, potentially leading to runaway feedback.

Let $\mathbf{s} = (s_1, s_2)^\top$, where s_1 and s_2 denote the position and velocity of a particle moving in one dimension. The SDI is written in state space form as

$$d\mathbf{s} = \left(\begin{bmatrix} 0 & 1 \\ 0 & -\gamma \end{bmatrix} \mathbf{s} + \begin{bmatrix} 0 \\ 1 \end{bmatrix} y \right) dt + \begin{bmatrix} 0 \\ \alpha \end{bmatrix} dW \quad (14)$$

$$\mathbf{x} = \mathbf{s} + \beta \epsilon \quad (15)$$

with $\epsilon \sim \mathcal{N}(\mathbf{0}, \mathbf{I})$. Here, α represents process noise, β represents observation noise and γ represents a friction term. Note that we again employ an OU process to model the stochastic dynamics of the velocity. The reward is given by a (negative) quadratic cost $r = -0.5\|\mathbf{x}\|^2 - 0.5y^2$. The agent is defined by $y = \theta^\top \mathbf{x}$ with learning dynamics given by Equations (8) and (9), as before. Note that the output y of the agent is the control input to the SDI whereas the SDI determines the observations \mathbf{x} of the agent. Hence, both the agent and the environment are modelled as coupled dynamical systems.

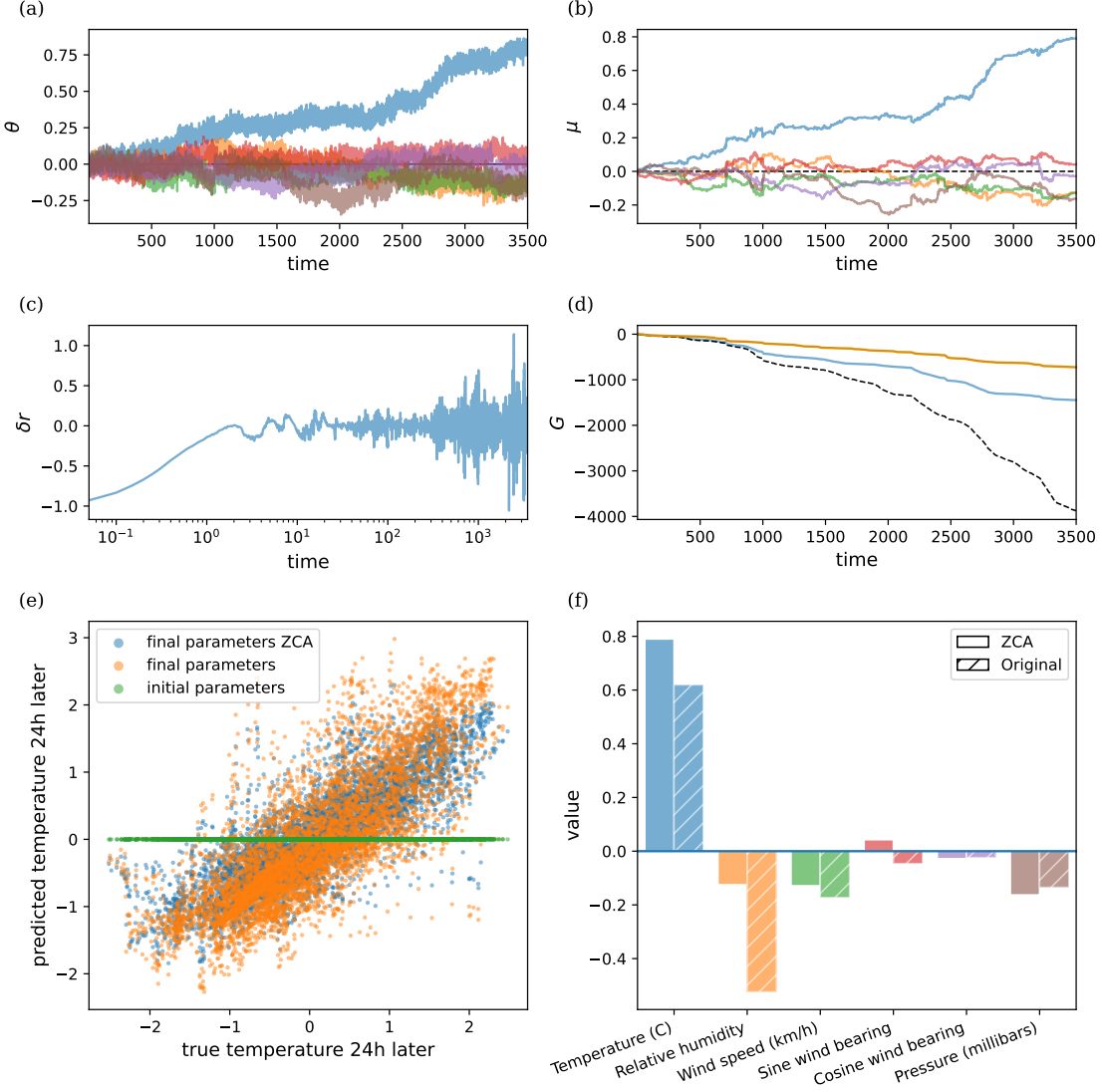


Figure 6: Dynamics of the weather prediction model whose parameters $\boldsymbol{\theta} = (\theta_1, \dots, \theta_6)$ denote current temperature, humidity, wind speed, sine of wind direction angle, cosine of wind direction angle and humidity, respectively. The goal is to learn to predict the temperature 24 hours later. Hyper-parameters are given by $\rho = 2$, $\lambda = 1$, $\sigma = 0.04$ and $\eta = 1$. Initial conditions are given by $\bar{r} = 0$, $\boldsymbol{\theta}_0 \sim \mathcal{N}(\mathbf{0}, 10^{-6} \mathbf{I})$ and $\boldsymbol{\mu}_0 = \boldsymbol{\theta}_0$. Initial conditions and optimal conditions are indicated by dashed and dotted lines, respectively. a) Dynamics of the parameters $\boldsymbol{\theta}$. b) Dynamics of the means $\boldsymbol{\mu}$. c) Dynamics of the reward prediction error $\delta r = r - \bar{r}$. Time variable shown on a logarithmic axis to visualise initial convergence. d) Return G as a function of time. Higher is better. The blue line indicates the return during parameter learning. The dashed line denotes the return when $\boldsymbol{\theta}$ is fixed to its initial state $\boldsymbol{\theta}_0$. The orange line indicates the return obtained when we fix parameters to the final mean parameters $\boldsymbol{\theta}(t) = \boldsymbol{\mu}(T)$ and use these during inference. e) True versus predicted 24h-ahead temperature on hold-out test data when using either the final estimated parameters $\boldsymbol{\mu}(T)$ with and without ZCA or the initial parameters $\boldsymbol{\theta}_0$. f) Estimated parameter values for each of the six regressors. In case of the original data, we report the final mean $\boldsymbol{\mu}(T)$ whereas for the whitened data we report $\boldsymbol{\mu}(T)\mathbf{R}$ as this projects the coefficients back into the original (correlated) space.

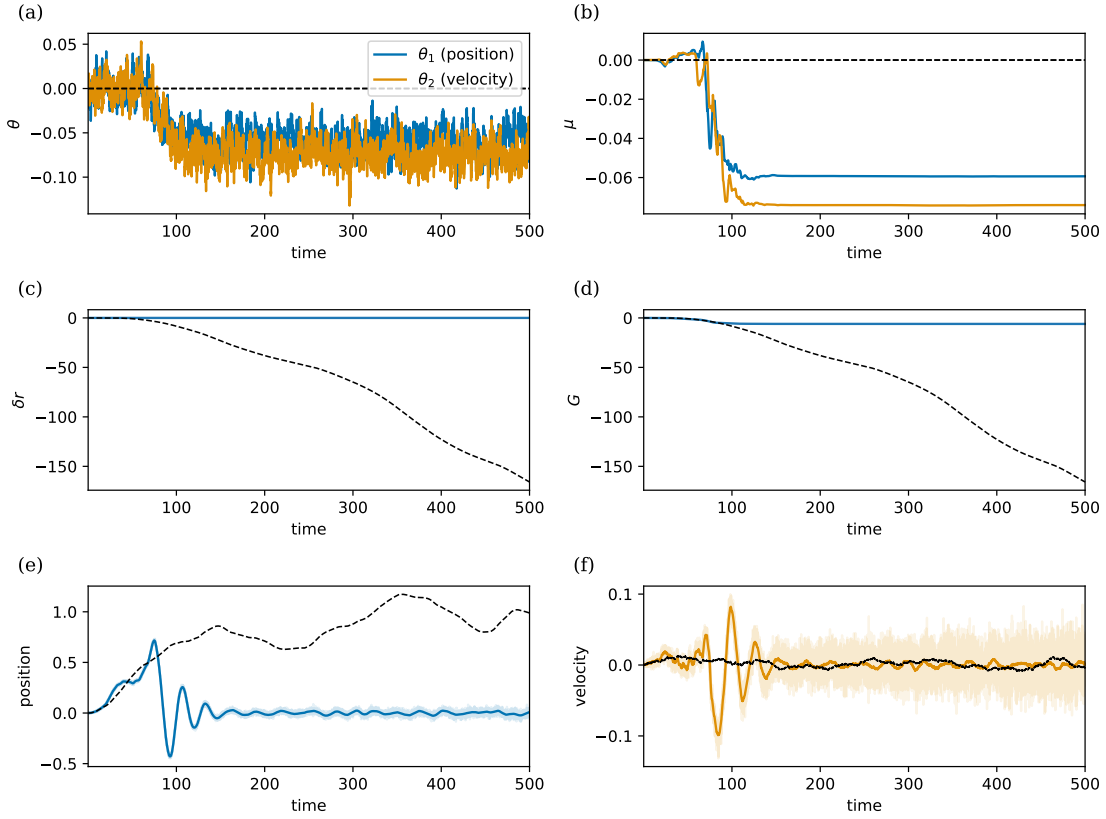


Figure 7: Learning to control a stochastic double integrator. Hyper-parameters are given by $\rho = 2$, $\lambda = 1$, $\sigma = 0.02$, $\eta = 50$, $\gamma = 0.01$ and $\rho = \omega = 0.001$. Initial conditions are set to zero for all variables. Initial conditions are indicated by dashed lines. a) Dynamics of the parameters θ . b) Dynamics of the means μ . c) Dynamics of the reward prediction error $\delta r = r - \bar{r}$. d) Return G as a function of time. Higher is better. The blue line indicates the return during parameter learning. The dashed line denotes the return when θ is fixed to its initial state θ_0 . e) Particle position after learning indicated in blue with observation noise indicated in light blue. The dashed line shows the change in the position in the absence of learning due to stochastic fluctuations in the velocity. f) Particle velocity after learning indicated in orange with observation noise indicated in light orange. The dashed line shows stochastic fluctuations in the velocity in the absence of learning.

Figure 7 shows that OUA can learn to control a stochastic double integrator, demonstrating effective learning in this more challenging control setting. Both the parameters for the position and the velocity converge to negative values. This is indeed optimal since it induces accelerations that move the particle's position and velocity to zero.

3.6 Meta-learning

In the previous analyses, we estimated θ and μ while keeping the hyper-parameters fixed. We may instead choose to learn the hyper-parameters as well using the same mechanism. Specifically, let us consider a learnable diffusion coefficient σ for the single-parameter model. We can see this as a form of meta-learning since modulation of σ changes the learning dynamics depending on the

problem at hand [51]. To implement meta-learning, we define additional equations

$$d\sigma = \lambda^\sigma(\mu^\sigma - \sigma) dt + \rho dW \quad (16)$$

$$d\mu^\sigma = \eta^\sigma \delta r(\sigma - \mu^\sigma) dt \quad (17)$$

with W a standard Wiener process, analogous to Equation (8) and (9).

To verify that the meta-learning process effectively identifies the optimal value for the chosen hyperparameter, in this case σ , we test OUA in a volatile environment where the target parameter θ^* switches from +1 to -1 during learning.

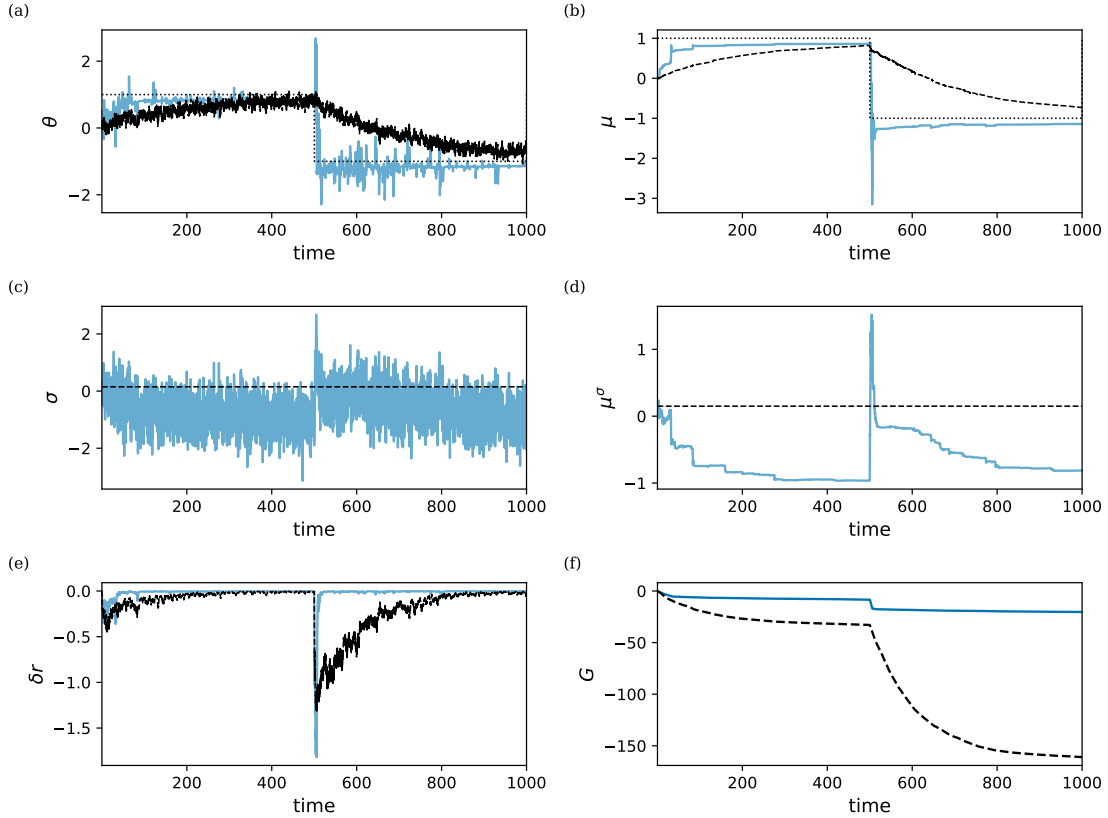


Figure 8: Results when using a learnt σ compared to using a constant $\sigma = \sigma_0$. Parameters are set to $\rho = \lambda = \eta = 1$, $\lambda^\sigma = 2$, $\rho = 0.05$ and $\eta^\sigma = 10.0$ for the model with learnt σ . The initial conditions are given by $\bar{r} = \theta_0 = \mu_0 = 0$ and $\sigma_0 = \mu_0^\sigma = 0.25$. Dashed lines indicate results when using a constant σ . a) Dynamics of θ . b) Dynamics of μ . c) Dynamics of σ . d) Dynamics of μ^σ . e) Dynamics of \bar{r} . f) Dynamics of G .

Figure 8 illustrates the learning dynamics of σ under these volatile conditions. As shown in Figure 8a, the system achieves faster convergence to the optimal θ when meta-learning is used, compared to a fixed σ . Additionally, the figure demonstrates how σ adapts by increasing its value when θ changes, promoting exploration, and decreasing when the target remains stable, favouring exploitation. The faster convergence is also reflected by the larger return in Fig. 8f. Figures 8c and 8d show that σ and μ^σ rapidly adapt to a more suitable higher value of σ , encouraging fast exploration. At a later stage, we observe adaptation to a value of σ below the initial σ_0 value, encouraging exploitation.

4 Discussion

In this paper, we introduced Ornstein-Uhlenbeck adaptation as new mechanism for learning in brains and machines. Our results show that learning can emerge purely as a function of simulating the equations of motion of a system whose parameters follow an Ornstein-Uhlenbeck process whose mean values are dynamically updated by the global reward prediction error. We have shown that OUA can effectively learn single- and multi-parameter models in supervised as well as reinforcement learning settings. Moreover, the same approach can be used to train recurrent systems and meta-learn the hyper-parameters of the model, the latter providing an automated approach to optimally balance between exploration and exploitation [15, 59]. We hypothesize that, in this setting, the remaining drift of θ about its mean provides a useful approximation of the posterior distribution of θ as estimated in fully Bayesian settings [70].

Our approach has important implications for machine learning as it offers a gradient-free approach to learning. That is, in contrast to the backpropagation algorithm, no exact gradient information, no backward pass and no non-local information other than a global reward signal is needed. OUA is also extremely parallelizable since multiple agents may simultaneously explore parameter space using one global parameter mean μ . This may have implications for federated learning [36]. In our experiments, we show that learning stability depends on the choice of hyper-parameters (cf. Figure 3). Here, the use of meta-learning or black-box optimization techniques such as Bayesian optimization [55, 53] and evolution strategies [6] can be of value.

An important question that remains to be explored is how well OUA scales to extremely large problems as currently used in machine learning. Such scaling may be facilitated by several factors. First, rather than using Wiener processes, we may want to exploit other noise processes like (compound) Poisson processes. The latter have the advantage that only a small set of weights is updated each time, preventing entanglement of weight updates, though at the expense of longer training times that are needed to exhaustively sample weight space. Second, as shown in Figure 6, decorrelating the input data through ZCA whitening aids convergence. It has been shown that decorrelation can be exploited as a general approach to speed up learning [2, 1], even in deep and recurrent networks [11, 17]. Note that in our setup, deep networks can be interpreted as recurrent networks with block-diagonal structure, allowing their direct integration into the proposed framework. The decorrelation update itself can even be formulated as part of the forward dynamics using local operations only [1], again providing a mechanism for biologically-plausible learning. Apart from scaling, we argue that local learning in lower-dimensional settings is of key importance as well, e.g., as a mechanism for adapting arbitrary machine learning models over time through a small number of learnable (hyper-)parameters.

Our work also has important implications for biology as it points towards a potential mechanism for noise-based learning in the brain [14]. We postulate that stochastic release of neurotransmitters [8, 47] in the synaptic cleft may be the brain’s way to search for potentially more effective synaptic weight values. Our theory suggests that this must then be accompanied by some mechanism which dynamically adjusts the average neurotransmitter release depending on a global (dopaminergic) reward prediction error signal. Note that our approach is similar in spirit to reward-modulated Hebbian learning (RMHL), where the proposed update of a weight θ_{ij} connecting a pre-synaptic neuron j to postsynaptic neuron i is a function of the reward prediction error and the activity difference of a neuron with respect to its mean activity [29]. Formally, RMHL can be seen as a biologically plausible version of node perturbation [22, 69, 65, 18, 11, 17] whereas OUA can be seen as a biologically plausible version of weight perturbation [71, 10, 12].

Our work is also of particular relevance for neuromorphic computing and other (non-von-Neumann-style) unconventional computing approaches [34, 50, 57, 43, 33, 40, 62], where the aim is to realise learning and inference as emerging from the physics [23, 24]. These approaches provide a route towards sustainable energy-efficient intelligent systems. Our approach merely requires that systems adapt their parameter values online via appropriate drift and diffusion terms that are realisable by physical components. This is very different from current practice in AI, where learning and inference are viewed as separate. Note further that OUA is ideally suited for training event-driven (spiking) neuromorphic systems [54] since we do not rely on differentiability of the

model.

We postulate that in next-generation AI systems, intelligence should emerge purely from running a system’s equations of motion forward in time, if they are to be efficient and effective. We demonstrated how this can be achieved using local operations in dynamical systems by exploiting the mean-reverting property of the Ornstein-Uhlenbeck process. Future work will focus on further theoretical analysis of our approach, extending our approach towards high-dimensional settings, considering other challenging cases such as delayed rewards or catastrophic forgetting, and implementing OUA in neuromorphic hardware and other unconventional computing platforms.

Acknowledgments

This publication is part of the DBI2 project (024.005.022, Gravitation), which is financed by the Dutch Ministry of Education (OCW) via the Dutch Research Council (NWO).

References

- [1] Nasir Ahmad. Correlations are ruining your gradient descent. *ArXiv preprint arXiv:2407.10780*, 2024.
- [2] Nasir Ahmad, Ellen Schrader, and Marcel van Gerven. Constrained parameter inference as a principle for learning. *ArXiv preprint arXiv:2203.13203*, 2022.
- [3] Anthony J Bell and Terrence J Sejnowski. The “independent components” of natural scenes are edge filters. *Vision Research*, 37(23):3327–3338, 1997.
- [4] Guillaume Bellec, Franz Scherr, Anand Subramoney, Elias Hajek, Darjan Salaj, Robert Legenstein, and Wolfgang Maass. A solution to the learning dilemma for recurrent networks of spiking neurons. *Nature Communications*, 11(1):3625, 2020.
- [5] Yoshua Bengio. How auto-encoders could provide credit assignment in deep networks via target propagation. *ArXiv preprint arXiv:1407.7906*, 2014.
- [6] Hans-Georg Beyer and Hans-Paul Schwefel. Evolution strategies – a comprehensive introduction. *Natural Computing*, 1:3–52, 2002.
- [7] Elie L Bienenstock, Leon N Cooper, and Paul W Munro. Theory for the development of neuron selectivity: orientation specificity and binocular interaction in visual cortex. *Journal of Neuroscience*, 2(1):32–48, 1982.
- [8] Tiago Branco and Kevin Staras. The probability of neurotransmitter release: variability and feedback control at single synapses. *Nature Reviews Neuroscience*, 10(5):373–383, 2009.
- [9] Steven L Brunton and J Nathan Kutz. *Data-Driven Science and Engineering: Machine Learning, Dynamical Systems, and Control*. Cambridge University Press, 2022.
- [10] Gert Cauwenberghs. A fast stochastic error-descent algorithm for supervised learning and optimization. *Advances in Neural Information Processing Systems*, 5, 1992.
- [11] Sander Dalm, Joshua Offerdeld, Nasir Ahmad, and Marcel van Gerven. Efficient deep learning with decorrelated backpropagation. *ArXiv preprint arXiv:2405.02385*, 2024.
- [12] A. Dembo and T. Kailath. Model-free distributed learning. *IEEE Transactions on Neural Networks*, 1(1):58–70, 1990.
- [13] J L Doob. The Brownian movement and stochastic equations. *Annals of Mathematics*, 43, 1942.

- [14] A A Faisal, L P J Selen, and D M Wolpert. Noise in the nervous system. *Nature Reviews Neuroscience*, 9:292–303, 2008.
- [15] A A Feldbaum. Dual control theory, i. *Avtomat. i Telemekh.*, 21:1240–1249, 1960.
- [16] Chrisantha T Fernando, Anthony ML Liekens, Lewis EH Bingle, Christian Beck, Thorsten Lenser, Dov J Stekel, and Jonathan E Rowe. Molecular circuits for associative learning in single-celled organisms. *Journal of the Royal Society Interface*, 6(34):463–469, 2009.
- [17] Jesús García Fernández, Sander Keemink, and Marcel van Gerven. Gradient-free training of recurrent neural networks using random perturbations. *Frontiers in Neuroscience*, 18:1439155, 2024.
- [18] Ila R Fiete and H Sebastian Seung. Gradient learning in spiking neural networks by dynamic perturbation of conductances. *Physical Review Letters*, 97(4):048104, 2006.
- [19] Barry Flower and Marwan Jabri. Summed weight neuron perturbation: An $O(n)$ improvement over weight perturbation. *Advances in Neural Information Processing Systems*, 5, 1992.
- [20] Monica Gagliano, Vladyslav V Vyazovskiy, Alexander A Borbély, Mavra Grimonprez, and Martial Depczynski. Learning by association in plants. *Scientific Reports*, 6(1):38427, 2016.
- [21] Paul Haider, Benjamin Ellenberger, Laura Kriener, Jakob Jordan, Walter Senn, and Mihai A Petrovici. Latent equilibrium: A unified learning theory for arbitrarily fast computation with arbitrarily slow neurons. *Advances in Neural Information Processing Systems*, 34:17839–17851, 2021.
- [22] Naoki Hiratani, Yash Mehta, Timothy Lillicrap, and Peter E Latham. On the stability and scalability of node perturbation learning. *Advances in Neural Information Processing Systems*, 35:31929–31941, 2022.
- [23] Herbert Jaeger, Beatriz Noheda, and Wilfred G. van der Wiel. Toward a formal theory for computing machines made out of whatever physics offers. *Nature Communications 2023* 14:1, 14:1–12, 2023.
- [24] C. Kaspar, B. J. Ravoo, W. G. van der Wiel, S. V. Wegner, and W. H.P. Pernice. The rise of intelligent matter. *Nature*, 594:345–355, 6 2021.
- [25] Patrick Kidger. *On Neural Differential Equations*. PhD thesis, University of Oxford, 2021.
- [26] David B Kirk, Douglas Kerns, Kurt Fleischer, and Alan Barr. Analog VLSI implementation of multi-dimensional gradient descent. *Advances in Neural Information Processing Systems*, 5, 1992.
- [27] Dhiresha Kudithipudi, Mario Aguilar-Simon, Jonathan Babb, Maxim Bazhenov, Douglas Blackiston, Josh Bongard, Andrew P. Brna, Suraj Chakravarthi Raja, Nick Cheney, Jeff Clune, Anurag Daram, Stefano Fusi, Peter Helfer, Leslie Kay, Nicholas Ketz, Zsolt Kira, Soheil Kolouri, Jeffrey L. Krichmar, Sam Kriegman, Michael Levin, Sandeep Madireddy, Santosh Manicka, Ali Marjaninejad, Bruce McNaughton, Risto Miikkulainen, Zaneta Navratilova, Tej Pandit, Alice Parker, Praveen K. Pilly, Sebastian Risi, Terrence J. Sejnowski, Andrea Soltoggio, Nicholas Soures, Andreas S. Tolias, Darío Urbina-Meléndez, Francisco J. Valero-Cuevas, Gido M. van de Ven, Joshua T. Vogelstein, Felix Wang, Ron Weiss, Angel Yanguas-Gil, Xinyun Zou, and Hava Siegelmann. Biological underpinnings for lifelong learning machines. *Nature Machine Intelligence 2022* 4:3, 4:196–210, 3 2022.
- [28] Yann Lecun, Yoshua Bengio, and Geoffrey Hinton. Deep learning. *Nature*, 521:436–444, 2015.
- [29] Robert Legenstein, Steven M Chase, Andrew B Schwartz, and Wolfgang Maass. A reward-modulated hebbian learning rule can explain experimentally observed network reorganization in a brain control task. *Journal of Neuroscience*, 30(25):8400–8410, 2010.

[30] Timothy P Lillicrap, Adam Santoro, Luke Marris, Colin J Akerman, and Geoffrey Hinton. Backpropagation and the brain. *Nature Reviews Neuroscience*, 21(6):335–346, 2020.

[31] Seppo Linnainmaa. The representation of the cumulative rounding error of an algorithm as a Taylor expansion of the local rounding errors. *Master’s Thesis (in Finnish), Univ. Helsinki*, pages 6–7, 1970.

[32] D Lippe and Joshua Alspector. A study of parallel perturbative gradient descent. *Advances in Neural Information Processing Systems*, 7, 1994.

[33] Víctor López-Pastor and Florian Marquardt. Self-learning machines based on Hamiltonian echo backpropagation. *Physical Review X*, 13:031020, 8 2023.

[34] Danijela Markovic, Alice Mizrahi, Damien Querlioz, and Julie Grollier. Physics for neuromorphic computing. *Nature Reviews Physics*, 2:499–510, 2020.

[35] Henry Markram, Joachim Lübke, Michael Frotscher, and Bert Sakmann. Regulation of synaptic efficacy by coincidence of postsynaptic aps and epsps. *Science*, 275(5297):213–215, 1997.

[36] H. Brendan McMahan, Eider Moore, Daniel Ramage, Seth Hampson, and Blaise Aguera y Arcas. Communication-efficient learning of deep networks from decentralized data. In *Proceedings of the 20th International Conference on Artificial Intelligence and Statistics (AISTATS)*, volume 54, pages 1273–1282. PMLR, 2017.

[37] Carver Mead. Neuromorphic electronic systems. *Proceedings of the IEEE*, 78:1629–1636, 1990.

[38] Thomas Miconi. Biologically plausible learning in recurrent neural networks reproduces neural dynamics observed during cognitive tasks. *Elife*, 6:e20899, 2017.

[39] Dharmendra S Modha, Rajagopal Ananthanarayanan, Steven K Esser, Anthony Ndirango, Anthony J Sherbondy, and Raghavendra Singh. Cognitive computing. *Communications of the ACM*, 54:62–71, 2011.

[40] Ali Momeni, Babak Rahmani, Matthieu Malléjac, Philipp del Houne, and Romain Fleury. Backpropagation-free training of deep physical neural networks. *Science*, 11 2023.

[41] Nicholas P Money. Hyphal and mycelial consciousness: The concept of the fungal mind. *Fungal Biology*, 125(4):257–259, 2021.

[42] James Morrill, Patrick Kidger, Lingyi Yang, and Terry Lyons. Neural controlled differential equations for online prediction tasks. *ArXiv preprint arXiv:2106.11028*, 2021.

[43] Mitsumasa Nakajima, Katsuma Inoue, Kenji Tanaka, Yasuo Kuniyoshi, Toshikazu Hashimoto, and Kohei Nakajima. Physical deep learning with biologically inspired training method: gradient-free approach for physical hardware. *Nature Communications*, 13:1–12, 12 2022.

[44] Erkki Oja. Simplified neuron model as a principal component analyzer. *Journal of Mathematical Biology*, 15:267–273, 1982.

[45] Alexandre Payeur, Jordan Guerguiev, Friedemann Zenke, Blake A Richards, and Richard Naud. Burst-dependent synaptic plasticity can coordinate learning in hierarchical circuits. *Nature Neuroscience*, 24(7):1010–1019, 2021.

[46] Venkatesh G Rao and Dennis S Bernstein. Naïve control of the double integrator. *IEEE Control Systems Magazine*, 21(5):86–97, 2001.

[47] Edmund T Rolls and Gustavo Deco. *The Noisy Brain: Stochastic Dynamics as a Principle of Brain Function*. Oxford University Press, 2010.

[48] David E Rumelhart, Geoffrey E Hinton, and Ronald J Williams. Learning internal representations by error propagation. Technical report, California Univ San Diego La Jolla Inst for Cognitive Science, 1985.

[49] Hiroyuki Sasakura and Ikue Mori. Behavioral plasticity, learning, and memory in *c. Elegans*. *Current Opinion in Neurobiology*, 23(1):92–99, 2013.

[50] Benjamin Scellier and Yoshua Bengio. Equilibrium propagation: Bridging the gap between energy-based models and backpropagation. *Frontiers in Computational Neuroscience*, 11:24, 2017.

[51] Jürgen Schmidhuber. *Evolutionary Principles in Self-Referential Learning*. PhD thesis, 1987.

[52] Wolfram Schultz, Peter Dayan, and P Read Montague. A neural substrate of prediction and reward. *Science*, 275(5306):1593–1599, 1997.

[53] Bobak Shahriari, Kevin Swersky, Ziyu Wang, Ryan P Adams, and Nando De Freitas. Taking the human out of the loop: A review of Bayesian optimization. *Proceedings of the IEEE*, 104(1):148–175, 2015.

[54] Mahyar Shahsavari, David Thomas, Marcel A. J. van Gerven, Andrew Brown, and Wayne Luk. Advancements in spiking neural network communication and synchronization techniques for event-driven neuromorphic systems. *Array*, 20, 2023.

[55] Jasper Snoek, Hugo Larochelle, and Ryan P Adams. Practical Bayesian optimization of machine learning algorithms. *Advances in Neural Information Processing Systems*, 25, 2012.

[56] James C Spall. Multivariate stochastic approximation using a simultaneous perturbation gradient approximation. *IEEE Transactions on Automatic Control*, 37(3):332–341, 1992.

[57] Menachem Stern, Daniel Hexner, Jason W. Rocks, and Andrea J. Liu. Supervised learning in physical networks: From machine learning to learning machines. *Physical Review X*, 11, 6 2021.

[58] Richard S Sutton. *Reinforcement Learning: An Introduction*. A Bradford Book, 2018.

[59] Richard S. Sutton and Andrew G Barto. *Reinforcement Learning: An Introduction*. The MIT Press, 2nd edition, 2015.

[60] Belinda Tzen and Maxim Raginsky. Neural stochastic differential equations: Deep latent Gaussian models in the diffusion limit. *ArXiv preprint arXiv:1905.09883*, 2019.

[61] George E Uhlenbeck and Leonard S Ornstein. On the theory of the Brownian motion. *Physical Review*, 36(5):823–841, 1930.

[62] Eveline R. W. Van Doremale, Tim Stevens, Stijn Ringeling, Simone Spolaor, Marco Fattori, and Yoeri van de Burgt. Hardware implementation of backpropagation using progressive gradient descent for in situ training of multilayer neural networks. *Science Advances*, 10:8999, 7 2024.

[63] Yi Wan, Abhishek Naik, and Richard S Sutton. Learning and planning in average-reward markov decision processes. In *International Conference on Machine Learning*, pages 10653–10662. PMLR, 2021.

[64] P Werbos. *Beyond Regression: New Tools for Prediction and Analysis in the Behavioral Sciences*. PhD thesis, 1974.

[65] Justin Werfel, Xiaohui Xie, and H Seung. Learning curves for stochastic gradient descent in linear feedforward networks. *Advances in Neural Information Processing Systems*, 16, 2003.

- [66] James CR Whittington and Rafal Bogacz. An approximation of the error backpropagation algorithm in a predictive coding network with local Hebbian synaptic plasticity. *Neural Computation*, 29(5):1229–1262, 2017.
- [67] James CR Whittington and Rafal Bogacz. Theories of error back-propagation in the brain. *Trends in Cognitive Sciences*, 23(3):235–250, 2019.
- [68] Bernard Widrow and Michael A Lehr. 30 years of adaptive neural networks: perceptron, madaline, and backpropagation. *Proceedings of the IEEE*, 78(9):1415–1442, 1990.
- [69] Ronald J Williams. Simple statistical gradient-following algorithms for connectionist reinforcement learning. *Machine Learning*, 8:229–256, 1992.
- [70] Winnie Xu, Ricky T Q Chen, Xuechen Li, and David Duvenaud. Infinitely deep Bayesian neural networks with stochastic differential equations. *ArXiv:2102.06559v4 [stat.ML]*, 2022.
- [71] Paul Züge, Christian Klos, and Raoul-Martin Memmesheimer. Weight versus node perturbation learning in temporally extended tasks: Weight perturbation often performs similarly or better. *Physical Review X*, 13(2):021006, 2023.